Jpn. J. Appl. Phys. Vol. 33 (1994) pp. 966–970
Part 1, No. 2, February 1994

Temperature Dependence of Quantized States in Strained-Layer $In_{0.21}Ga_{0.79}As$/GaAs Single Quantum Well

Wuh-Sheng CHI, Ying-Sheng HUANG, Hao QIANG[1], Fred H. POLLAK[1],
David G. PETTIT[2] and Jerry M. WOODALL[2]
Department of Electronic Engineering, National Taiwan Institute of Technology, Taipei 106, Taiwan, ROC
[1]*Physics Department, Brooklyn College of CUNY, Brooklyn, NY 11210, USA*
[2]*IBM Thomas J. Watson Research Center, Yorktown Heights, NY 10598, USA*

(Received August 19, 1993; accepted for publication November 20, 1993)

The piezoreflectance (PzR) and photoreflectance (PR) measurements of a strained-layer (001) $In_{0.21}Ga_{0.79}As$/GaAs single quantum well as a function of temperature in the range of 20 to 300 K have been carried out. A careful analysis of the PzR and PR spectra has led to the identification of various excitonic transitions, mnH(L), between the mth conduction band state to the nth heavy (light)-hole band state. The parameters that describe the temperature dependence of $E_{\mathrm{mnH(L)}}$ are evaluated. The detailed study of the temperature variation of excitonic transition energies indicates that the main influence of temperature on quantized transitions is through the temperature dependence of the band gap of the constituent material in the well. The temperature dependence of the linewidth of the 11H exciton is evaluated and compared with that of the bulk material.

KEYWORDS: strained-layer $In_xGa_{1-x}As$/GaAs single quantum well, piezoreflectance, photoreflectance, temperature dependence of quantized states

1. Introduction

During the past few years there has been considerable interest in the strained layer in the $In_xGa_{1-x}As$/GaAs system from both fundamental and applied points of view.[1–6] Strained-layer heterostructures utilize constituent layers with unequal lattice constants. When the thickness of the layers is below a critical value, lattice mismatch can be accommodated by elastic strain and thus the growth of dislocation-free structures can be achieved.[7] This freedom greatly increases the ability to control the optical and electronic properties of such structures. For thin layers grown pseudomorphically, the strain induces a significant change in the electronic band structure. This makes it possible to control the band gap and associated quantum transitions by altering the ternary composition and layer thickness. Advantages of such a strained-layer system include band-gap tailoring for long-wavelength lasers[1] as well as the exploitation of the light in-plane hole effective mass and high electron speed for two-dimensional electron-gas field-effect transistors.[8]

Modulation spectroscopy, particularly piezoreflectance (PzR) and photoreflectance (PR), is shown to be a very powerful technique to study a large number of quantized states in a single quantum well (SQW) structure. Both PzR and PR spectra exhibit derivative-like features[9,10] in the vicinity of the intersubband excitonic transitions. Recently Tober *et al.* reported PzR as a supplement to PR for nondestructive characterization of GaAs/$Al_xGa_{1-x}As$ multiple quantum wells (MQWs).[11] In this paper we report a detailed study of the temperature dependence of the PzR and PR spectra from a strained-layer (001) $In_{0.21}Ga_{0.79}As$/GaAs SQW in the range of 20 to 300 K. Both the allowed and forbidden transitions mnH(L) have been observed. The notation mnH(L) denotes transitions between the mth conduction to the nth valence subband of heavy (H)- or light (L)-hole character. Comparison of the PzR and PR spectra has led to the identification of various excitonic transitions. The transition energies are extracted from the PzR spectra using a form of the Aspnes equation of the first-derivative Lorentzian line shape (FDLL),[12,13] while the PR spectra are fitted with the first-derivative Gaussian line shape (FDGL).[9,10]

The temperature dependence of the quantized transition energies $E_{\mathrm{mnH(L)}}$ have been studied in terms of a Bose-Einstein expression.[14,15] The results indicate that the main influence of temperature on the quantized transitions is through the temperature dependence of the band gap of the constituent material in the well. The temperature variation of the broadening parameter of 11H, $\Gamma_{11\mathrm{H}}(T)$, has been fitted to a Bose-Einstein-type expression.[14] The obtained intrinsic linewidth, Γ_0, of about 1.9 meV is the theoretical limit for random alloy scattering.[16] This indicates the high quality of the structure since there is no contribution due to strain distribution or interface roughness. The electron-optical phonon coupling term, Γ_1, for SQW is considerably smaller than that of the bulk materials.

2. Experimental

The SQW was fabricated by molecular beam epitaxy (MBE) in a Varian Gen-II system. The undoped (001) GaAs substrate was degreased, then etched in the solution of H_2SO_4, H_2O_2, and H_2O, mixed in the ratio of 12:1:1 by volume and quenched in water. When loaded, the substrate was thermally cleaned at 610°C, and growth of undoped GaAs at 1 μm/h was initiated. The saturated value of the arsenic tetramer beam-equivalent pressure was between 15 and 20 times that of the gallium during the growth. Before the 0.5 μm undoped buffer was completed, the substrate temperature was lowered so that the remaining third of the buffer, as well as the undoped SQW and 1 μm undoped GaAs cap, were grown at 580°C without interruption or change in source temperature. The growth conditions indicated an indium composition of 20% and a well width of 100 Å.

PzR was achieved by mounting the sample on a 0.15-

cm-thick lead zirconate titanate piezoelectric transducer driven by a 300 V_{rms} sinusoidal wave at 397 Hz. This produced a modulated strain in the sample of about 10^{-5} rms value. The PR apparatus has been described in the literature.[14] A 5 mW He–Ne laser, chopped at 197 Hz, was used as the modulating source and 100 W tungsten-halogen lamp filtered by a model 270 McPherson monochromator provided the monochromatic light. The laser intensity was reduced to about 1% to 10% of its initial value by using a neutral density filter. The reflected light was detected using an EG & G type HUV-4000B silicon photodiode. To facilitate the simultaneous measurement of both the PzR and PR spectra, a second lock-in amplifier was added, which had a reference channel derived from the piezoelectric transducer power supply. PzR and RR signals were obtained simultaneously and under identical experimental conditions. A RMC model 22 closed-cycle cryogenic refrigerator equipped with the model 4075 digital thermometer controller was used for the temperature-dependent measurements.

The X-ray scattering measurements were made using $CuK\alpha_1$ radiation from a Rigaku RU-300 generator operated at 15 kW. The specular (002 and 004) and nonspecular (224 and 404) reflections from the $In_xGa_{1-x}As$ layer and from the GaAs substrate were measured using a double-axis configuration of a Huber 5020 six-circle horizontal sample goniometer with both Ge(002) and perfect Si(111) monochromator crystals. The measured positions of the specular and nonspecular $In_xGa_{1-x}As$ reflections relative to the corresponding GaAs substrate reflections were used to determine the perpendicular ($a_\perp$) and parallel ($a_{/\!/}$) lattice constants of the $In_xGa_{1-x}As$ layer. The perpendicular lattice constant $a_\perp=5.805\pm0.004$ Å was calculated from the measured perpendicular momentum transfer components of the specular and nonspecular reflections. The parallel lattice constant of the $In_xGa_{1-x}As$ layer, calculated from the in-plane momentum transfer components of the nonspecular reflections, was identical to that of the GaAs substrate, $(a_{/\!/}-a_{GaAs})/a_{GaAs}=(5\pm6)\times10^{-4}$, indicating that the $In_xGa_{1-x}As$ layer is fully pseudomorphic with the GaAs substrate. From the observed finite size broadening of the $In_xGa_{1-x}As$ reflections, the thickness of the $In_xGa_{1-x}As$ layer was calculated to be $L=118\pm10$ Å. The fractional In composition calculated from the measured lattice constant, assuming simple elastic behavior of the $In_xGa_{1-x}As$ layer and that its Poisson's ratio is 0.31, is $x=0.204\pm0.010$.

3. Line Shape Considerations

The normalized change in the reflectivity measured in the PzR or PR experiment is related to the modulated dielectric function $\varepsilon(=\varepsilon_1+i\varepsilon_2)$ by[9,17]

$$\Delta R/R=\alpha(\varepsilon_1, \varepsilon_2)\Delta\varepsilon_1+\beta(\varepsilon_1, \varepsilon_2)\Delta\varepsilon_2, \quad (1)$$

where α and β are the Seraphin coefficients. The quantities $\Delta\varepsilon_1$ and $\Delta\varepsilon_2$ are the changes in the real and imaginary parts of the dielectric function, respectively, induced by the applied periodic stress or the modulating electric field created by the pump beam. It has been shown that for bound states such as excitons or the confined states of a quantum well, the change of the dielectric function $\Delta\varepsilon$ exhibits a first-derivative spectrum.[9,17] For excitons the dielectric function will have either a Lorentzian or Gaussian profile depending on whether the broadening is homogeneous or inhomogeneous, respectively. For the case of FDLL the modulated signal can be expressed as[9,10,17]

$$\Delta R/R=\mathrm{Re}\left\{\sum_j^n\left[C_je^{i\theta_j}(E-E_j+i\Gamma_j)^{-2}\right]\right\}, \quad (2)$$

where n is the total number of features, E is the photon energy, and C_j, θ_j, E_j, and Γ_j are the amplitude, phase, transition energy, and broadening parameters, respectively, for the jth feature. The simple form of eq. (2) neglects intensity modulation effects.[9,17] The expression for the change of the dielectric function $\Delta\varepsilon$ of a Gaussian profile does not have the simple analytical form of eq. (2).[9,10] For the case of two-dimensional band-to-band transitions, the dielectric function ε is given by[17]

$$\varepsilon\sim\ln(E-E_j+i\Gamma_j). \quad (3)$$

It has been reported that the FDLL is relevant for the PzR signal,[12,13] while the FDGL yields a better fit for PR spectra. We emphasize, however, that the positions of the quantum-confined transition energies extracted from such fits are relatively insensitive to the line shape function.

4. Results and Discussion

In Figs. 1(a), 1(b), and 1(c), the solid lines represent the experimental PzR and PR spectra at 300 K, 80 K and 20 K, respectively. The dashed lines are least-squares fits to the first-derivative line shape functions. The obtained values of the various intersubband energies at 300 K, 80 K, and 20 K are indicated by arrows at the bottom of the figures. It is interesting to note that at 80 K and 20 K the linewidth of the 11H transition has become sufficiently narrow so that 11H and 12H are clearly resolved. The 21H and 11L signals are also resolved at both temperatures. The fine structures in the spectra such as 13H, 22H and 23H signals, which are not well resolved at 300 K, are distinguished in the low-temperature spectra. Thus we could obtain more information than that from the room temperature spectrum. The presence of 12H and 23H, which are "symmetry-forbidden" transitions, is probably due to a small built-in electric field in the sample. Although 13H is "symmetry-forbidden", it is "parity allowed" because of the finite depth of the well. In addition, we have observed the development of two unidentified features located between 13H and 21H, and 23H and 22L. These two structures cannot be accounted for by the finite-well calculation. The reasons for the assignment of the PzR and PR peaks to the particular transitions shown in Figs. 1(a), 1(b), and 1(c) are discussed below.

From both PzR and PR spectra, we obtained consistent transition energies. In order to identify the origins of the various spectral features we performed a theoret-

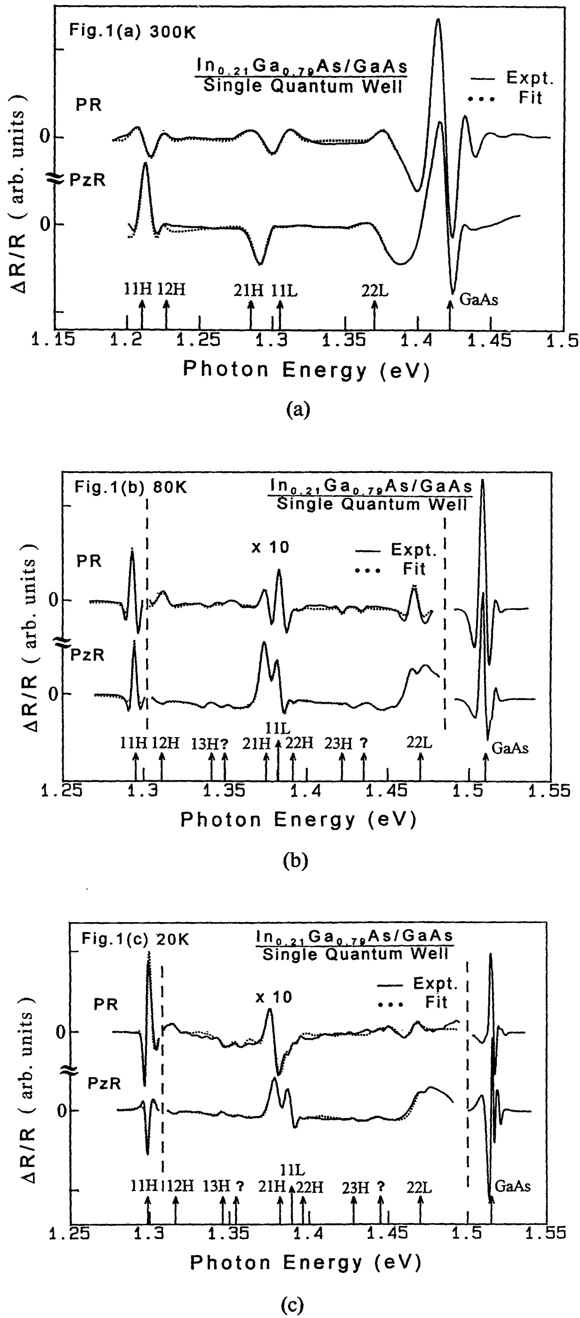

Fig. 1. Experimental piezoreflectance and photoreflectance spectra (solid lines) at (a) 300 K, (b) 80 K, and (c) 20 K, respectively. The dotted lines are least-squares fits to the first-derivative line shape functions (FDLL for PzR and FDGL for PR).

ical calculation based on the envelope function model,[18] including the exciton binding energy[19] and the effects of strain.[2-4] The strains at 300 K and 20 K are 1.505% and 1.514%, respectively. At low temperatures, the additional strain induced by differences in linear expansion coefficients may be neglected since this value is less than 0.6% of strain at 300 K. We have used a number of relevant parameters of $In_xGa_{1-x}As$ listed in ref. 20. The lattice constant (a), hydrostatic (A) and shear (B) deformation potentials, and the stiffness constants (C_{11} and C_{12}) of the ternary material were obtained by linear interpolation of values of the end-point semiconductors GaAs and InAs listed in Table I. The best fit was obtained for an indium composition of 0.21 ± 0.01, a well width of 105 ± 10 Å, and a conduction band offset ratio $Q_c=0.63\pm0.03$. PzR and PR are reported to exhibit selective[11] and nonselective modulation spectra, respectively, where the PzR technique is relatively sensitive to the light-hole transition. From a direct comparison of the PzR and PR spectra, unambiguous indentifications of light- and heavy-hole exciton transitions are made. Another aid in our interpretation of Figs. 1(a), 1(b), and 1(c) is the recent work of Qiang *et al.*[21] They studied the effects of uniaxial stress along the [100] direction on a similar sample. They were able to identify the heavy- and light-hole features from their stress dependence.

Shown in Fig. 2 are the PzR spectra at different temperatures. The energy scale corresponds to the spectrum at 300 K. Other spectra have been shifted to align the 11H transition signal at 300 K (1.21 eV). The identifications are denoted by numbers below each curve and are described at the right side of the figure. There is no obvious change in each transition as temperature

Table I. Values of the lattice constants (a), the hydrostatic (A) and the shear (B) deformation potentials, and the stiffness constants (C_{11} and C_{12}) of GaAs and InAs.

Materials	a (Å)	A (eV)	B (eV)	C_{11} (10^{11} dyn/cm^2)	C_{12} (10^{11} dyn/cm^2)
GaAs	5.6533[20]	−8.7[23]	−2.0[23]	11.88[20]	5.32[20]
InAs	6.0584[20]	−5.8[25]	−1.8[25]	8.33[20]	4.53[20]

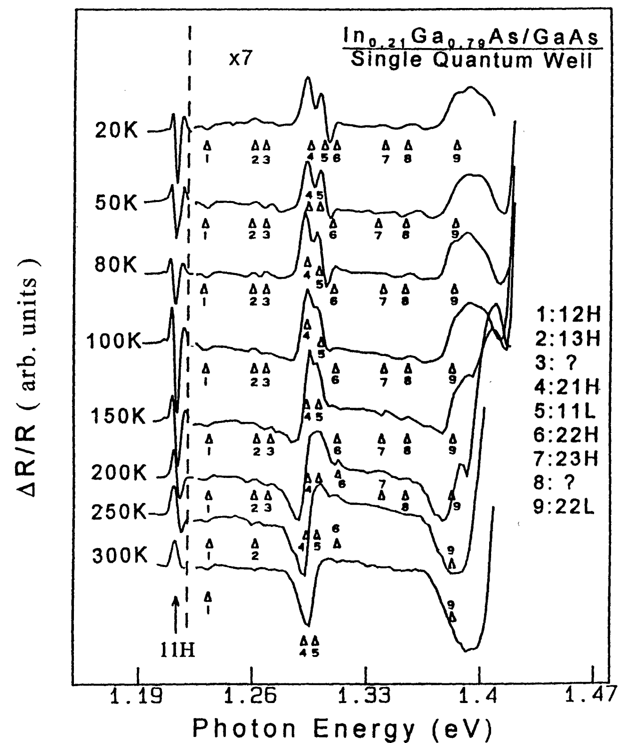

Fig. 2. Experimental piezoreflectance spectra at different temperatures. The energy scale corresponds to the spectrum at 300 K. Other spectra have been shifted to align 11H transition signals at 300 K (1.21 eV). The identifications are denoted by numbers below each curve and are described at the right side of the figure.

is varied. The solid lines in Fig. 3 are the least-squares fits to the Bose-Einstein expression given by Lautenschlager *et al.*:[14,15)]

$$E(T)=E_B-a_B\{1+2/[\exp(\theta_B/T)-1]\}, \quad (4)$$

where $E(T)$ is the transition energy of mnH(L) at temperature T, a_B represents the strength of the electron-phonon interaction and θ_B corresponds to the average phonon temperature. Our values of E_B, a_B and θ_B are given in Table II, along with the corresponding values for the direct gaps (E_0) of GaAs[4)] and $In_xGa_{1-x}As$ ($x=0.06$ and $x=0.15$) bulks.[22)] The a_B and θ_B in our sample are fairly similar to those of $In_xGa_{1-x}As$ bulk. For light and heavy holes there are slight differences in estimates of a_B and θ_B. We interpret this as being the result of the different effective masses and their temperature dependence. Since the differences are within the probable errors of measurement, a detailed comparsion of these parameters is difficult to make. Therefore, as in the lattice-matched $Al_xGa_{1-x}As$/GaAs heterostructure system, the main influence of temperature on the quantized transitions is through the temperature dependence of the band gap of the constituent material in the well.[23,24)]

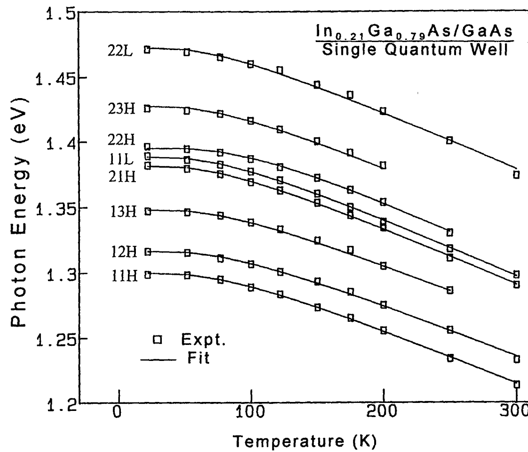

Fig. 3. Temperature dependence of the various excitonic transition energies. The solid lines are the least-squares fits to eq. (4).

Table II. Values of the parameters which describe the temperature dependence of mnH(L) transition energies of $In_xGa_{1-x}As$/GaAs SQW and energy gap of $In_xGa_{1-x}As$, GaAs bulks.

Materials		E_B (eV)	a_B (meV)	θ_B (K)
	11H	1.351±0.010	51±7	237±40
	12H	1.369±0.010	53±7	250±40
	13H	1.397±0.010	49±7	236±40
$In_{0.21}Ga_{0.79}As$/GaAs	21H	1.432±0.011	51±8	225±45
single quantum well	11L	1.442±0.011	52±8	216±45
	22H	1.448±0.012	51±9	235±47
	23H	1.479±0.012	51±9	226±47
	22L	1.523±0.015	51±10	220±50
$In_{0.06}Ga_{0.94}As$ bulk[22)]		1.466±0.014	44±9	203±45
$In_{0.15}Ga_{0.85}As$ bulk[22)]		1.339±0.015	53±10	238±50
GaAs[14)]		1.571±0.023	57±29	240±102

In Fig. 4 we display the temperature dependence of the broadening parameter Γ for the 11H transition, Γ_{11H}, as determined from the theoretical fit of the PR spectra. The solid line in Fig. 4 is a least-squares fit to the phonon-coupling model given by[14)]

$$\Gamma(T)=\Gamma_0+\Gamma_1/[\exp(E_{ph}/kT)-1], \quad (5)$$

where Γ_0 contains inhomogeneous contributions due to interface roughness, alloy clusterings, and strain distributions. The parameter Γ_1 represents the strength of electron-optical phonon coupling while E_{ph} is the energy of the longitudinal optical phonon.[22)] The values of Γ_0, Γ_1 and E_{ph} are listed in Table III. Also displayed are recently reported values for similar SQWs[25)] and that of the direct gap for strain relieved $In_xGa_{1-x}As$/GaAs ($x=0.06$ and $x=0.15$).[22)] The value of Γ_0 is considerably smaller than those reported in ref. 22 for somewhat similar SQWs. Our value of about 1.9 meV is close to the theoretical limit for alloy scattering.[16)] This indicates the high structural quality of the material (uniform strain distribution) and interface, averaged over the region sampled by the exciton Bohr radius (~100 Å). The similarity of E_{ph} indicates that it is indeed the energy of the longitudinal optical phonon for this material. The value of Γ_1 for 11H of the SQW is considerably smaller than that of the direct gap E_0 for the bulk materials. This agrees well with a recent report[27)] on the size dependence of the electron-lon-

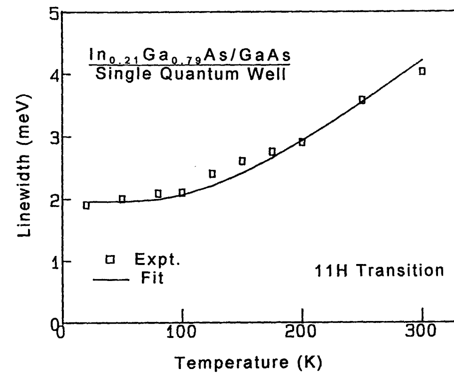

Fig. 4. Temperature dependence of the broadening parameter of the 11H transition. The solid line is a least-squares fit to eq. (5).

Table III. Values of the parameters Γ_0, Γ_1, and E_{ph} which describe the temperature dependence of the broadening parameter of 11H transition in single quantum wells and that of the direct gap for strain-relieved $In_xGa_{1-x}As$/GaAs.

Materials	Γ_0 (meV)	Γ_1 (meV)	E_{ph} (meV)
$In_{0.21}Ga_{0.79}As$/GaAs SQW (L=110 Å)	1.9±0.1	6.9±0.5	36±3
$In_{0.20}Ga_{0.80}As$/GaAs[26)] SQW (L=84 Å)	9	7	35
$In_{0.15}Ga_{0.85}As$/GaAs[26)] SQW (L=65 Å)	11.3	7	35
$In_{0.06}Ga_{0.94}As$/GaAs[22)]	7.5±0.5	23±6	31±10
$In_{0.15}Ga_{0.85}As$/GaAs[22)]	10.5±0.5	23±6	32±10

gitudinal optical phonon interaction for which the thermal broadening of the linewidth diminishes as the dimensions and the size of the system are reduced.

5. Conclusions

In conclusion, we have studied the various excitonic transitions of a high-quality strained-layer $In_{0.21}Ga_{0.79}As/GaAs$ SQW by PzR and PR techniques. Comparing the PzR and PR spectra has led to the identification of various excitonic transitions. A detailed study of the temperature variation of these excitonic transition energies, $E_{mnH(L)}(T)$, shows that the main influence of temperature on quantized transitions is through the temperature dependence of the band gap of the consituent material in the well. We have analyzed $E_{mnH(L)}(T)$ and $\Gamma_{11H}(T)$ in terms of the Bose-Einstein expression. The strength of the electron-phonon interaction and the average phonon temperature are similar to those of $In_xGa_{1-x}As/GaAs$ bulk, while the value of the strength of the electron-optical phonon coupling Γ_1 for 11H is considerably smaller than that of the direct gap E_0 for strain-relieved $In_xGa_{1-x}As$ material.

Acknowledgments

W. S. Chi and Y. S. Huang acknowledge the support of the National Science Council of the Republic of China. H. Qiang and F. H. Pollak acknowledge the partial support of US Army Research Office contract #DAAL03-92-G-0189.

1) W. T. Tsang: *Semiconductors and Semimetals*, ed. R. Dingle (Academic, New York, 1987) Vol. 24, p. 397.
2) S. H. Pan, H. Shen, Z. Huang, F. H. Pollak, W. Zhuang, Q. Xu, A. P. Roth, R. A. Masut, C. Lacelle and D. Morris: Phys. Rev. B **38** (1988) 3375.
3) G. Ji, W. Dobbelarer, D. Huang and H. Morkoc: Phys. Rev. B **39** (1989) 3216.
4) D. J. Arent, K. Deneffe, C. Van Hoof, J. DeBoeck and G. Borghs: J. Appl. Phys. **66** (1989) 1739.
5) P. W. Yu, G. D. Sanders, D. R. Evans, D. C. Reynolds, K. K. Bajaj, C. E. Stutz and R. L. Jones: Appl. Phys. Lett. **54** (1989) 2230.
6) A. Ksendzov, H. Shen, F. H. Pollak and D. P. Bour: Solid State Comm. **73** (1990) 11.
7) see, for example, J. W. Mayer and S. S. Lau: *Electronic Materials Science for Integrated Circuits in Si and GaAs* (Macmillan, New York, 1990) p. 425.
8) H. Morkoc and H. Unlu: *Semiconductors and Semimetals*, ed. R. Dingle (Academic Press, New York, 1987) Vol. 24, p. 135.
9) F. H. Pollak and O. J. Glembocki: Proc. SPIE **946** (1988) 2.
10) O. J. Glembocki and B. V. Shanabrook: Superlattice & Microstruct. **3** (1987) 235.
11) R. L. Tober, A. L. Smirl, T. F. Boggess and J. N. Schulman: J. Appl. Phys. **64**. (1988) 4678.
12) Y. R. Lee, A. K. Ramdas, L. A. Kolodziejski and R. L. Gunshor: Phys. Rev. B **38** (1988) 13143.
13) H. Mathieu, J. Allegre and B. Gil: Phys. Rev. B **43** (1991) 2218.
14) P. Lautenschlager, M. Garriga, S. Logothetidis and M. Cardona: Phys. Rev. B **35** (1987) 174.
15) P. Lautenschlager, M. Garriga, L. Vina and M. Cardona: Phys. Rev. B **36** (1987) 4821.
16) J. Singh and K. K. Bajaj: Appl. Phys. Lett. **48** (1986) 1077.
17) D. E. Aspnes: *Handbook on Semiconductors*, ed. T. S. Moss (North-Holland, New York, 1980) Vol. 2, p. 109.
18) G. Bastard and J. A. Brum: IEEE J. Quantum Electron. **QE-22** (1986) 1625.
19) K. J. Moore, G. Duggan, K. Woodbridge and C. Robert: Phys. Rev. B **41** (1990) 1090.
20) S. Adachi: J. Appl. Phys. **53** (1982) 8775.
21) H. Qiang, F. H. Pollak, C. Mailhiot, G. D. Pettit and J. M. Woodall: Surf. Sci. **267** (1992) 103.
22) Z. Hang, D. Yan, F. H. Pollak, G. D. Pettit and J. M. Woodall: Phys. Rev. B **44** (1991) 10546.
23) H. Qiang, F. H. Pollak and G. Hickman: Solid State comm. **76** (1990) 1087.
24) A. Kangarlu, H. R. Chandrasekher, M. Chandrasekhar, Y. M. Kapoor, F. A. Chambers, B. A. Vojak and J. M. Meese: Phys. Rev. B **37** (1988) 1035.
25) *Landolt-Bornstein New Series Group III*, ed. K. H. Hellwege (Springer-Verlag, Berlin, 1982) Vol. 179.
26) K. F. Huang, K. Tai, S. N. G. Chu and A. Y. Cho: Appl. Phys. Lett. **54** (1989) 2026.
27) H. Qiang and F. H. Polllak: Appl. Phys. Lett. **61** (1992) 1411.